The Pennsylvania State University

The Graduate School

College of the Liberal Arts

GENE EXPRESSION OF GROWTH PLATE FORMATION IN MOUSE METATARSALS

A Thesis in

Anthropology

by

Catherine Roberts

Submitted in Partial Fulfillment
of the Requirements
for the Degree of

Master of Arts

May 2018

The thesis of Catherine Roberts was reviewed and approved* by the following:

Philip Reno

Associate Professor of Bio-Medical Sciences

Thesis Advisor

Timothy Ryan

Associate Professor of Anthropology

Thesis Advisor

Ken Hirth

Professor of Anthropology

Graduate Program Director

*Signatures are on file in the Graduate School

ABSTRACT

Growth plates are structures which allow a bone to grow in length. The morphological evolution of the mammalian skeleton is characterized by changes in bone development, such as the loss or gain of growth plate formation in a particular bone. Differences in developmental processes are driven by differential gene expression both during organismal development and throughout their lifetime. This project uses mouse models to observe the genetic factors correlated with the presence or absence of growth plate formation in the metatarsal. The aim is to create a working list of genetic factors related to growth plate development.

TABLE OF CONTENTS

LIST OF FIGURES

LIST OF TABLES

ACKNOWLEDGEMENTS

To the Department of Anthropology,
professors and graduate students,
for believing in my abilities and for developing my understanding of the human experience

To the Reno Laboratory,
especially Philip Reno, Kelsey Kjosness, and Jasmine Hines,
for mentoring me and being patient with me through this learning process

To Audrey Chambers and Betty Blair,
for dealing with my chaotic schedule and making this degree possible

To Craig Praul of the Penn State Genomics Core Facility,
for overseeing the sequencing of our data

To Istvan Albert of the Penn State Bioinformatics Consulting Center,
for assisting with our data analysis

To Christina Bergey,
for helping troubleshoot my Galaxy problems and encouraging my development

To Devin Pohly,
for reviewing my personal statement and making me laugh when life was rough

INTRODUCTION

Evolutionary developmental biology seeks to understand how various morphological forms arise from existing structures and processes. Homologous patterns of development, such as the organizational structure and formation of bone, provide a framework in which novel traits can arise. Modifications arise within this framework and are subject to the evolutionary forces that allow these modifications to be lost or fixed in a species.

The skeletal system provides structure and support to vertebrate animals. This system manifests in variable morphologies along different evolutionary lineages. These morphologically distinct skeletons contribute to the various modes of locomotion, posture, and movement of different species. The processes through which bones form are generally similar in all vertebrates. However, the developmental patterning of particular limbs or bones widely varies. These modifications in phenotype are rooted in modifications of developmental patterning. The when and where of gene expression during development results in the differences seen between adult organisms (Müller and Newman 2003).

Growth plates are structures formed in vertebrate development that function to extend the length of a developing bone. A bone maintains a region of cartilage cells which continue to divide throughout development and allow the bone to grow in length (Gilbert 1991).

While leg and arm bones form two growth plates, metacarpals and metatarsals, the bones of the hands and feet, each form a single growth plate on only one end of the bone. The proximal end of the bone, which articulates with the wrist/ankle, is formed from the primary center diaphysis through direct ossification, while the distal end, which articulates with a proximal phalanx, forms a growth plate and a secondary center of ossification. This trait makes metacarpals and metatarsals ideal subjects for studying the processes underlying growth plate

formation. Cells from the same primary center are similar in developmental timing and environment, but some form a secondary center and a growth plate while others do not. They can, therefore, be directly compared in terms of the signals they receive. We expect that their gene expression levels would be similar. The difference in gene signaling factors present in these cells include those which are either inhibiting or promoting growth plate formation (Reno et al. 2006).

In this thesis project, I compare RNA sequence data from either end of developing metatarsals, with the aim of identifying the potential gene expression difference involved in their differential ossification and growth plate formation.

BACKGROUND

Growth Plate Formation

Many bones develop by a process known as endochondral ossification. Through this method, cartilaginous tissue calcifies and is replaced by bone. Cartilage cells (known as chondrocytes) release calcium to create an extracellular matrix. Osteoblasts use this matrix to replace the chondrocytes with bone cells. The process begins at the primary ossification center, at the midpoint of the bone, and extends outwards (Gilbert 1991). The chondrocytes are organized in layers, with more mature cells near the primary center, where calcification is occurring. In some bones, this ossification continues outwards from the primary center until all cartilage is replaced, and the bone is entirely formed.

However, in long bones, the ends begin to form their own (secondary) ossification centers, known as epiphyses. This happens as blood vessels enter the cartilage tissue at the ends of the bone and stimulate ossification before the osteoblasts at the primary center have reached the area. Instead of all the chondrocytes calcifying, some continue to replicate while others are maturing. This region, known as an epiphyseal plate, or growth plate, is organized into zones. As cells move towards the bone shaft, they proliferate, mature/grow, and calcify. These zones are visually distinctive due to the increase in cell size and organization of the cells into columns as they get closer to forming the extracellular matrix. The formation of a growth plate allows the bones to continue growing in length by generating new cartilage as older chondrocytes are ossified. Eventually new cartilage stops being formed and all the existing cartilage is replaced by bone, fusing the primary and secondary centers to form a single bone (Gilbert 1991).

Many processes and interactions contribute to the formation of growth plates. Any changes to the timing of these processes or loss/gain of growth plate formation alters the morphology of the developing individual. Morphogen patterns drive many aspects of skeletal formation and function. Cells undergo segregation, migration, and differentiation in response to morphogenic signals. While it is necessary to tease apart the factors and processes involved in each activity, this can be difficult due to the multitude of signals and responses, and the complexity of the networks involved.

Skeletal Evolution

Compared to the many quadrupedal vertebrates, primates have modifications to their forelimbs, especially hands and wrists, which allow for grasping movements. Much of what sets humans apart from other primates is our unique bipedal locomotion. Changes in forelimb and hind limb morphology can facilitate or constrain particular movements. Our first digit on the foot is aligned with the other toes, and many modifications to the legs allow for our center of mass to remain above the feet and our posture to remain upright (Müller and Newman 2003).

The skeletal system is a very plastic system. The development pattern of bones is driven by gene expression. Development, therefore, exists within the context of heritable genes and signaling patterns, but can also respond to external forces in the environment. Natural selection acts on phenotype, creating complex interplay between environment and genes. Determining genetic pathways involved in bone formation and development is a key step towards understanding skeletal evolution (Müller and Newman 2003).

Most mammals form two ossification centers in a particular carpal called the pisiform. Humans, however, do not, resulting in a reduced structure compared to other mammals. It is likely that a shift in the timing of signaling primary center formation plays a role in this change (Kjosness et al. 2014). A better understanding of the signals and pathways involved in bone formation will further aid in understanding these changes throughout evolutionary time.

Metatarsal Developmental Timing

The metatarsal was chosen for this study due to the two ossification processes present in its development. In a mouse, the growth plate on the distal end begins to form approximately at birth. At this time, patterning appears similar between the two ends, but with the distal end having an identifiable perichondrial ring and a proliferative reserve zone. By postnatal day 9, the cells on the distal end have differentiated into the zones which characterize a growth plate. At this same time, the zones on the proximal end have been obliterated and much of the cartilage has calcified to bone (See Figure 1).

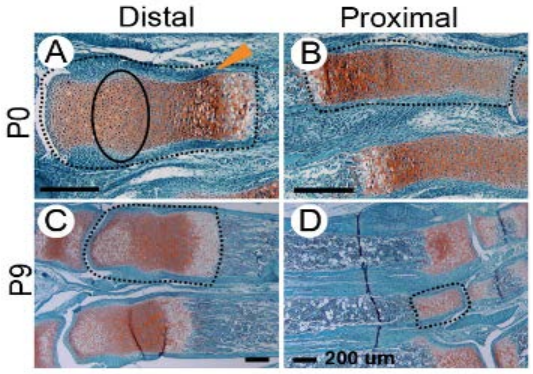

Figure 1. P0 and P9 Cell Patterning

(A) At birth, chondrocytes at the distal end is organized into zones with a perichondrial ring (orange arrow) and proliferative cell reserve, (black ring), while **(B)** similar chondrocyte zoning is seen at the proximal end. **(C)** On day 9, an organized growth plate has formed at the distal end, while **(D)** clear zones are no longer present on the proximal end and much of it has calcified.

Mouse *(Mus Musculus)* Models

Mice are widely used in biological studies. They are easy to obtain, and there exists a great deal of information and genomic data regarding their biology. Many mouse genes have already been connected to human homologs. As mammals, their metatarsal development is similar to our own. However, the growth plate on the pisiform bone was lost in humans since our divergence from chimpanzees, and mice, therefore, have growth plates whereas we do not (Kjosness et al. 2017). Because of this, our laboratory is obtaining data for both a bone with similar developmental patterning to our own and one with different patterning. This will allow us to account for species-specific expression in our exome comparisons.

Gene Expression in Functioning Growth Plates

The past few years have yielded many discoveries regarding the roles of gene expression in growth plate function and bone development. This section is a culmination of our current knowledge of gene expression involved in endochondral ossification and growth plate development.

Endochondral ossification begins with mesenchyme cell condensation. The active genes involved in this process mainly play a role in affecting molecules related to adhesion between cells. *Hoxa13* and *Hoxd13* knockouts affected Eph-ephrin signaling and, consequently, the cell-cell adhesion involved in sorting undifferentiated mesenchyme. In particular, the gene associated with defining the digits in undifferentiated limb mesenchyme, *EphA7*, experienced reduced expression in *Hoxa13* -/- embryos. Additionally, many congenital skeletal disorders are known to be caused by mutations in fibroblast growth factor receptors (FGFRs). *FGFR1* and *FGF2* are

both expressed in the limb bud mesenchyme prior to condensation, and a knockout of both caused a reduction in limb element growth. FGFRs are also involved in later chondrocyte maturation and hypertrophy (Long and Ornitz 2013).

Bone morphogenic protein (BMP) signaling also plays a role in cell coalescence and defining mesenchyme clusters. While not all developing regions respond equally to changes in *BMP2* and *BMP4* expression, deletion of BMP type I receptors resulted in the loss of many skeletal elements, namely most of those formed through endochondral ossification. This suggests a major role of BMP signaling in cartilage formation. Later in development, BMP2 and BMP4 play a role in osteoblast maturation (Long and Ornitz 2013).

After condensation, mesenchymal cells differentiate into various types of chondrocytes. While not necessary for the initial condensation step, Sox9 transcription factor is responsible for the differentiation of mesenchyme into chondrocytes, known as chondrogenesis. Loss of *Sox9* expression prevented any chondrogenesis in developing embryos. Sox9 also interacts with Sox5 and Sox6 to activate genes which code for components of the extracellular matrix. Alternatively, Wnt/β-catenin signaling pathways prevent chondrocyte differentiation. This signaling works in opposition to the factors promoting chondrogenesis (Long and Ornitz 2013).

Following differentiation, the chondrocytes undergo proliferation, maturation, and hypertrophy. The parathyroid hormone-related peptide receptor (*PTHR1*) gene is highly expressed in maturing chondrocytes but prior to hypertrophy. The parathyroid hormone-related peptide and its receptor prevent premature hypertrophy. The expression of the parathyroid hormone-related peptide (PTHrP) and Indian hedgehog (Ihh) exist on an axis, along which the zones related to growth plate organization are formed. *Ihh* is expressed both in chondrocytes just

before and just after hypertrophy. It stimulates chondrocyte proliferation, *PTHrP* expression, and chondrocyte transition from round to columnar (Long and Ornitz 2013).

Ihh is also necessary for osteoblast differentiation. This occurs through activation of the *RUNX2*, a gene which has been found to both promote chondrocyte hypertrophy and differentiate osteoblasts in the perichondrium. Hypertrophic chondrocytes express matrix metalloproteinase 13 (*MMP13*), which allows for vascularization of the surrounding extracellular matrix. Simultaneously, osteoblasts differentiate and enter the matrix, replacing the cartilage with bone (Long and Ornitz 2013).

There are many genes involved in the interactions between the aforementioned factors which have been identified, but there are many more questions left to be answered. There is much to be learned about how these factors interact to perform specific functions or create specific patterning. Little is known about the regulation of matrix vascularization and its timing. This is not only a crucial aspect of endochondral ossification but also of the formation of primary and secondary ossification centers, a defining feature which differentiates growth plate formation (Long and Ornitz 2013).

METHODS

This project involves collecting and sequencing RNA from the distal and proximal ends of mouse metatarsal samples. The data was sequenced, and statistical analyses were performed by the Huck Institute at The Pennsylvania State University and sent to our lab. I analyzed the results by utilizing the open-source bioinformatic tools provided by Galaxy.

RNA-seq

The tissue collection and RNA-extraction were performed by the Reno Lab. Metatarsals were collected from wild type FVB/NJ mice at P0, P4 and P9. These stages correspond to periods where skeletal elements are undergoing growth plate patterning (P0), initial stages of ossification and preliminary growth plate formation (P4), and primary center nearly fully ossified with an active growth plate (P9) (See Figure 1) (Reno et al. 2006). The cartilaginous portions of the distal and proximal ends from the third metatarsal were collected and pooled for each litter. Three litters were collected for each age to serve as experimental replicates. This allows us to eliminate genes that only happen differ in expression in one individual at a particular age point. A minimum of three repeats is an accepted number for ensuring the reliability of the p-values and the ability to make conclusions about *Mus musculus* development (Conesa et al. 2016).

For RNA extraction, the metatarsals are dissected in ice cold RNAlater (Life Technologies). Total RNA was extracted using a TissueLyserII (Qiagen) and RNeasy Microarray Tissue Mini Kit (Qiagen), and cDNA libraries were constructed using RT2 First Strand Kit (Qiagen) (Wang et al. 2011, Zheng and Cohn 2011). Sample quality was assessed using an Agilent Bioanalyzer and those with RNA Integrity Numbers (RIN) > 9 were be submitted to the

Penn State's Genomics Core Facility for sequencing. Samples were sequenced on an Illumina HiSeq 2500 two lane Rapid Run mode using 150 nt single read sequencing producing 33 – 40 million reads per sample.

Galaxy

The internet platform Galaxy provides a variety of tools for the analysis of genetic data. These tools allow users to assemble, trim, and align sequences and perform various statistical tests all in one place. Developed here, at Penn State, Galaxy (biostar.usegalaxy.org) is an open-source project that is free to use.

The RNA sequences with which I worked were mostly in FASTQ format. This file format holds transcript sequence data and quality scores for each base pair. Galaxy provides a converter for FASTQ files, as different sequencing machines have different ways of organizing the information. This converter modifies the data to make it readable by other tools in Galaxy.

For this project, I used the tools provided by Galaxy to compare RNA-seq data between proximal and distal cartilage cells to determine if there is a significant difference in gene expression between the two sites. This involved aligning each RNA sequence with a template genome for the purpose of identifying each gene. I then pooled the data from all three samples and compared the expression levels between the two sites. All of the tools necessary to complete this process are part of the open source Tuxedo software suite, which includes the TopHat and Cufflinks packages, and are accessible through Galaxy (Trapnell et al. 2012).

TopHat aligned each RNA-seq genome (in FASTQ format) with an annotated *Mus musculus* genome (UCSC annotated mm10). This sequence data is free to use, and complete

annotation sets for dozens of animal species and assemblies are available. The software examined the mapped reads and determined the locations of splice junctions. TopHat generated BAM files containing location information in relation to the template genome from the existing FASTQ sequence data. For some age categories, the sequencing center already provided BAM files. These were used for comparison to ensure the validity of the TopHat results and consistent experiment replication (Trapnell et al. 2012).

The Cufflinks tool set enables both assembling transcripts and comparing gene expression data. Cuffdiff2 (See Cuffdiff2 section) uses a combination of statistical models to address the many confounding variables of differential expression testing. Cuffdiff2 and DESeq are the two tools used to calculate significance values for this project.

Statistical Approaches

The aim of this project is to determine likely growth plate forming factors from mouse exome data. The nature of this hypothesis calls for analysis of variance testing. This method compares the variation seen in the expression data from the distal ends of the metatarsals with that of the proximal ends to determine if the difference between the two is significant. A natural variance occurs in gene expression as well as some expected sampling error. Analysis of variance takes these factors into account and calculates the likelihood that the difference in expression between the two metatarsal structures is due to an additional, driving force (Roff 2006).

However, there is no generally accepted standard method for this sort of biological data. A principle components analysis will cluster similar data together, revealing the level of

variability within a site. This can then be used to determine the significance of the differences between sites. In statistical data, a small percentage of significant genes are false positives. However, due to the large scale of genomic (in this case, exomic) data, a small percentage is calculated out to be thousands of genes. Statistical software attempts to correct for much of this error. Additionally, the use of many samples from different individuals in this project helps to eliminate false positives (Conesa et al. 2016).

Zhang, et al. (2014) describe many of the challenges in determining differentially expressed genes. They mention biases related to varying lengths of transcripts, nucleotide composition, replicates, depth of sequencing coverage, gene isoforms, and overlapping transcripts, in addition to variation within and between groups which may confound detection of differentially expressed genes. The expected variation of gene expression within and between organisms has not been fully explored nor has the difference in expected variation between two loci. While modern bioinformatics software continues to progress and improve in its ability to account for these factors, there is still much debate over the proper analytical methods to be used for comparative exome data.

A variety of tools exist for differential expression testing. As such, my results varied depending on the software I used and the statistical methods utilized by each program. Each will provide different results based on the assumptions they make and how they approach normalizing the results. Much of the early literature describes the use of Bayesian or Poisson models in RNA-seq analysis. Current software tools favor modified negative binomial models.

A reasonable q-value cap, or false discovery rate, can be difficult to determine. Again, it is difficult to know how much fluctuation to expect between individuals and across different age groups. Overall, $q < 0.05$ seems to be a reasonable limit. Any lower and we risk eliminating

important candidates. The q-value is already developed with the intention of eliminating false positives. The use of multiple samples tries to account for some error and allows for some fluctuation in expression over developmental time. Merely the presence of three samples, instead of two or one, allows for vastly greater confidence in our results than we would have otherwise (Conesa et al. 2016).

Cuffdiff2

Cuffdiff2 uses a modification of a Poisson model. The Poisson model tends to be restrictive, with the observed data having greater variation than predicted by the model, and does not account for ambiguity in the data. Cuffdiff2 attempts to address both these issues through a combination of a negative binomial model and a beta distribution. The negative binomial model estimates the variability in the data (the degree of overdispersion of the Poisson model) and uses this information to estimate fragment counts. Additionally, the Cuffdiff2 algorithm aims to account for the large amount of sequences that are similar between different genes and the high amount of variability in count data. Cuffdiff2 uses a beta distribution to calculate and assign uncertainty values to the fragment count for each transcript. The Cuffdiff2 algorithm incorporates both of these models, estimating a count variance for each transcript and aiming to account for both the variation in the data and the ambiguity in mapping fragments. This individualized transcript variance within one sample is accounted for when comparing two datasets (Trapnell, et al. 2013).

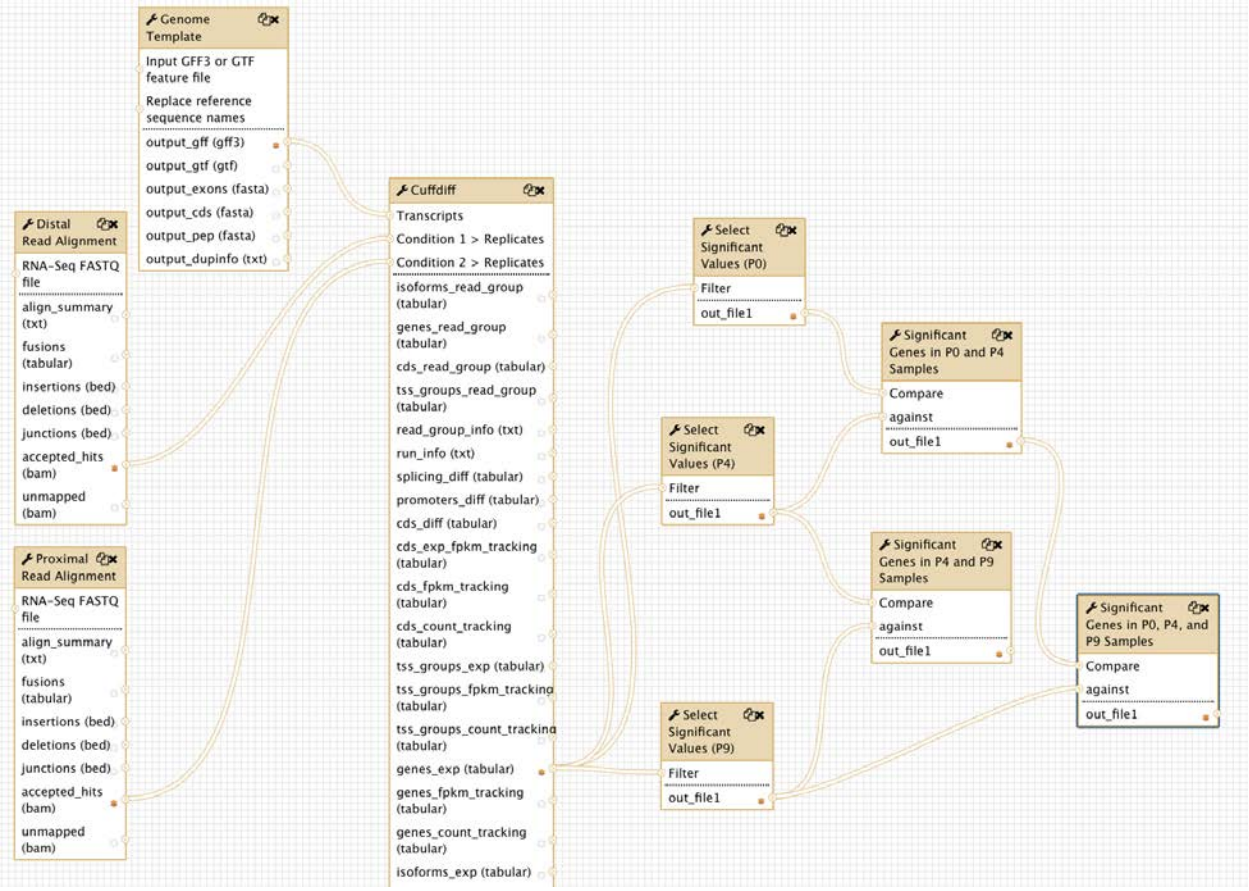

Figure 2. Galaxy Workflow

The Cuffdiff tool receives the inputs of distal and proximal bam reads and the mm10 genome template and compares expression at each gene to determine adjusted p-values for each locus. This output is then filtered, eliminating those with high q-values (> 0.05). This is repeated for the other two age groups and the tables of 'significant' genes for each age are compared to one another.

DESeq

Like Cuffdiff, the DESeq tool bases its statistical analysis on the negative binomial model. DESeq is an R package distributed through the open-source Bioconductor project. The Huck Institute at Penn State performed the data sequencing as well as a DESeq analysis. Rather than using BAM files, DESeq uses count matrix input (Zhang, et al. 2014). It uses assumptions to estimate the mean and variance from the data (Anders and Huber 2010). P-values were tabulated for each gene, and genes with adjusted p-values less than 0.05 at both ages P0 and P9

are presented in Table 3. Compared to other software packages, DESeq is conservative in its calculations, yielding fewer false positives but also fewer true positives (Soneson and Delorenzi 2013).

Integrative Genome Viewer

Developed at the Broad Institute, the Integrative Genome Viewer (IGV) is a program which combines sequence visualization with other genomic tools. IGV allows us to view expression level data and eliminate genes with irregular expression patterning, likely caused by sampling error. It enables visualization of input data across different scales, from the entire chromosome to quantitative values on a single piece of a gene. Aligned with the corresponding genes from a sample template, levels of expression are shown for each base pair, forming a graph of expression levels across each gene. Tracks can be added to show differentially expressed genes on each chromosome. The zoom feature allows the user to view the expression in each sample down to the transcribed regions of the gene (Robinson et al. 2011).

The purpose of using IGV was to provide a visualization of the expression levels at each gene and to detect abnormalities in expression levels. IGV is especially useful in its ability to detect outliers. Outliers can skew the data if their values too great, such that their high expression levels outweigh the other two samples. IGV assists outlier identification by placing the graphs of the data next to one another and allowing the user to scale the graphs to one another (Robinson et al. 2011). Figure 2 provides an example of an outlier. In Litter A, the proximal sample shows significantly higher expression of *Lcn2*. None of the other proximal samples show the same heightened expression levels.

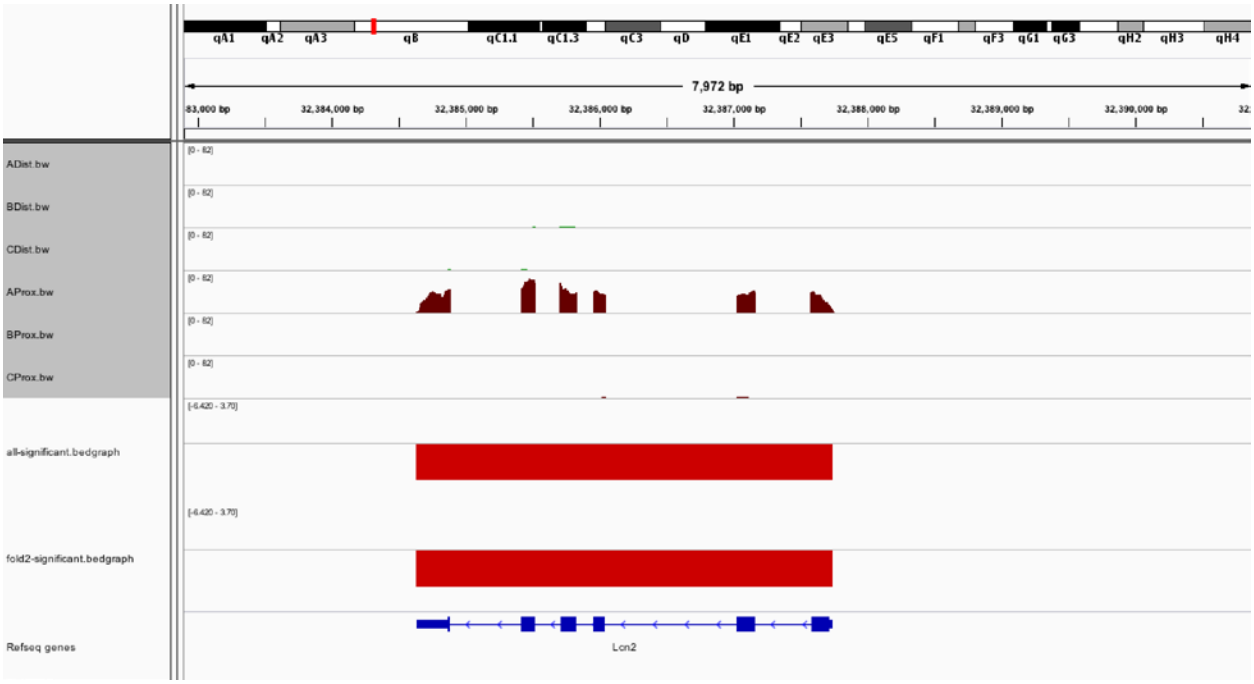

Figure 3. Expression Outlier in Proximal A Sample

We also found two of the samples had been switched along the way, AProximalP0 and ADistalP0. This is clear from looking at the expression of a gene across many samples. When all of the proximal samples show heightened expression, the one distal P0 sample does as well, while the proximal sample does not. In Figure 4, five proximal samples show high *Sall1* expression levels, along with one distal sample (ADistP0), and five distal samples show low Sall1 expression, along with one proximal sample (AProxP0). Therefore, these samples were corrected, and the analyses were redone. This error certainly affected the results and would have been difficult to detect without the Integrative Genome Viewer.

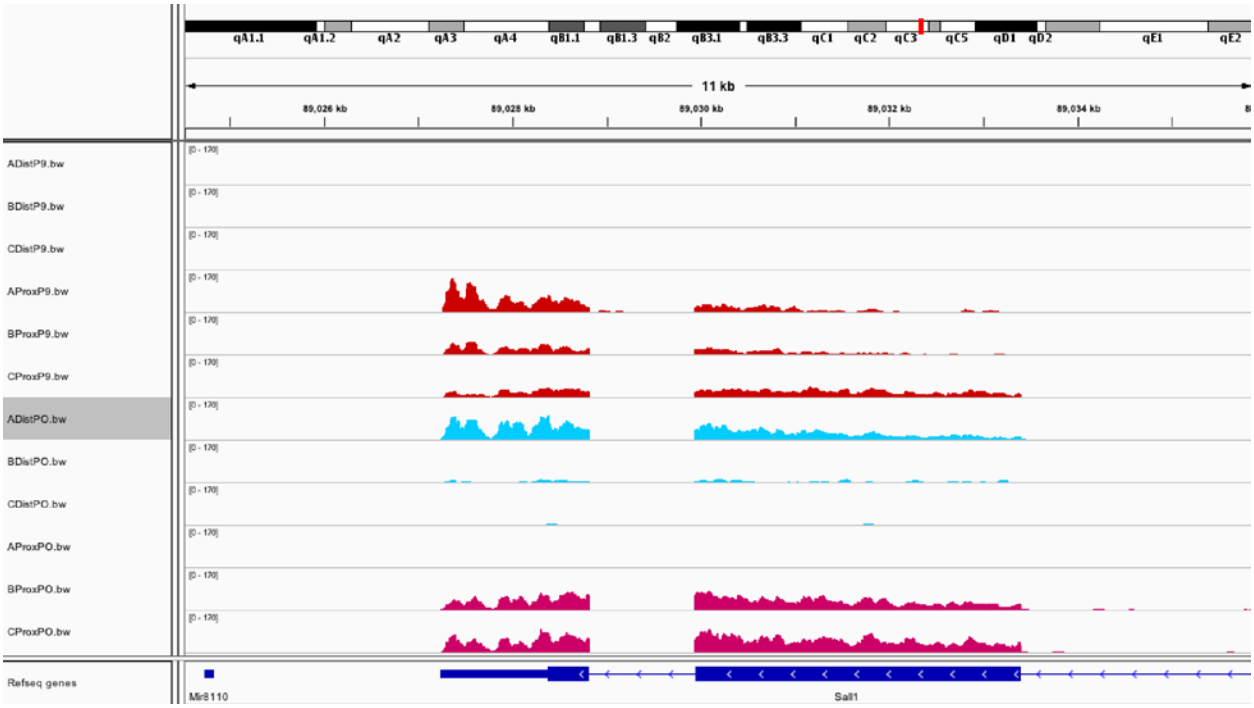

Figure 4. Distal Sample (ADistP0) Aligns with Proximal Sample Patterns

RESULTS

Table 1. Differentially expressed genes (q<0.05) across all ages (P0, P4, and P9), generated by Galaxy pipeline (see Figure 2), and their corresponding locations on the mm10 genome

Gene Name	*Location on mm10 genome*
A230065H16Rik	chr12:111406808-111412077
Acta1	chr8:123891757-123894775
Actc1	chr2:114047283-114052875
Actn2	chr13:12269426-12340732
Adam22	chr5:8072346-8368160
Adgrd1	chr5:129096749-129204599
Agtr2	chrX:21484623-21488833
Apcdd1	chr18:62922326-62953195
Apod	chr16:31296191-31314808
Atp1a2	chr1:172271708-172298064
Bnc2	chr4:84272541-84675086
Car3	chr3:14863537-14872373
Casq2	chr3:102086454-102146512
Chit1	chr1:134111241-134151540
Chst11	chr10:82985496-83195891
Clu	chr14:65968482-65981548
Cpm	chr10:117629499-117687352
Crabp1	chr9:54764747-54773110
Crabp2	chr3:87948692-87953372
Cxcl14	chr13:56288642-56296551
Ddn	chr15:98803781-98807925
Egfl6	chrX:166523006-166585716
Enpep	chr3:129269176-129332749
Epha3	chr16:63545217-63864157
Erg	chr16:95359168-95586593
Eya1	chr1:14168957-14310199

Fbln1	chr15:85206007-85286294
Fndc1	chr17:7738567-7804974
Foxc1	chr13:31806645-31810635
Gdf6	chr4:9844371-9862345
Gldn	chr9:54268579-54341777
Gpnmb	chr6:49036517-49058182
H2-DMa	chr17:34122831-34139101
Hbb-b1	chr7:103826522-103827929
Ihh	chr1:74945314-74951672
Itgb1bp2	chrX:101449108-101453541
Lbp	chr2:158306492-158332852
Lonrf2	chr1:38794508-38821215
Ltbp2	chr12:84783211-84879755
Magel2	chr7:62376978-62381640
Mal	chr2:127633225-127656695
Me1	chr9:86581362-86701253
Megf6	chr4:154170712-154275721
Mepe	chr5:104325328-104338611
Miat	chr5:112213227-112228948
Moxd1	chr10:24223516-24302783
Mpz	chr1:171150712-171161130
Myl1	chr1:66924295-66945056
Mylpf	chr7:127211607-127214287
Ntn4	chr10:93641048-93745972
Ntrk3	chr7:78192113-78577838
Papss2	chr19:32595714-32667187
Pi16	chr17:29318881-29328902
Pknox2	chr9:36890978-37147322
Pla2g7	chr17:43568450-43612201
Plppr4	chr3:117319145-117360876
Ppp2r2c	chr5:36868569-36955078
Prrx1	chr1:163245118-163313650

Ptpru	chr4:131768456-131838278
Ptprv	chr1:135108497-135132575
Sall1	chr8:89027242-89044162
Sbspon	chr1:15853861-15892722
Scin	chr12:40059770-40134228
Sfrp1	chr8:23411501-23449632
Slc16a3	chr11:120948483-120959000
Sost	chr11:101962457-101967015
Stc1	chr14:69029288-69041401
Steap1	chr5:5736321-5749317
Stk39	chr2:68210446-68471981
Stra6	chr9:58129087-58153997
Svep1	chr4:58042795-58206596
Tbx2	chr11:85832614-85841948
Tnn	chr1:160085031-160153575
Tnnc1	chr14:31208311-31211711
Tnnc2	chr2:164777161-164779734
Tnni1	chr1:135799420-135810989
Trabd2b	chr4:114406723-114615098
Ttc22	chr4:106622448-106640187
Tubb3	chr8:123411563-123422010
Vwf	chr6:125552947-125686679
Wipf3	chr6:54452882-54503768
Wnt10a	chr1:74792018-74804175
Wnt16	chr6:22288226-22298522
Wnt5a	chr14:28505472-28525515
Xylt1	chr7:117380978-117667630
Zfp185	chrX:72987338-73031543

Table 2. Differentially expressed genes (q<0.05) and their corresponding q-values calculated for each age group, generated by the Galaxy pipeline (see Figure 2)

Gene Name	*P0 q-value*	*P4 q-value*	*P9 q-value*
A230065H16Rik	0.00322311	0.000557471	0.00279654
Acta1	0.0395251	0.000557471	0.00279654
Actc1	0.00322311	0.000557471	0.00279654
Actn2	0.0155242	0.000557471	0.00483895
Adam22	0.00322311	0.000557471	0.0186021
Adgrd1	0.00322311	0.000557471	0.00279654
Agtr2	0.00322311	0.000557471	0.00279654
Apcdd1	0.00322311	0.000557471	0.00483895
Apod	0.00322311	0.000557471	0.00279654
Atp1a2	0.0078259	0.000557471	0.0116048
Bnc2	0.00322311	0.000557471	0.00279654
Car3	0.00322311	0.000557471	0.00279654
Casq2	0.00322311	0.000557471	0.0211005
Chit1	0.00322311	0.00104026	0.00279654
Chst11	0.0155242	0.000557471	0.00279654
Clu	0.00322311	0.000557471	0.00279654
Cpm	0.00322311	0.000557471	0.0116048
Crabp1	0.00322311	0.000557471	0.00279654
Crabp2	0.00322311	0.000557471	0.00279654
Cxcl14	0.00322311	0.000557471	0.0103526
Ddn	0.0496274	0.00147973	0.0116048
Egfl6	0.00322311	0.000557471	0.00279654
Enpep	0.00322311	0.000557471	0.00279654
Epha3	0.00322311	0.000557471	0.00279654
Erg	0.00322311	0.000557471	0.0266697
Eya1	0.00322311	0.000557471	0.0354346
Fbln1	0.0174222	0.000557471	0.0116048
Fndc1	0.0118497	0.00230771	0.00483895

Foxc1	0.0248749	0.000557471	0.0255991
Gdf6	0.0469437	0.000557471	0.00867114
Gldn	0.00322311	0.000557471	0.00279654
Gpnmb	0.00564358	0.000557471	0.0435794
H2-DMa	0.00322311	0.000557471	0.00279654
Hbb-b1	0.0190842	0.000557471	0.0247866
Ihh	0.0078259	0.00104026	0.0425509
Itgb1bp2	0.0118497	0.000557471	0.0197755
Lbp	0.0118497	0.000557471	0.00279654
Lonrf2	0.00322311	0.000557471	0.00867114
Ltbp2	0.0100722	0.000557471	0.00279654
Magel2	0.00322311	0.000557471	0.00279654
Mal	0.0207794	0.000557471	0.0103526
Me1	0.00322311	0.000557471	0.0376833
Megf6	0.00322311	0.000557471	0.00483895
Mepe	0.0137262	0.00271116	0.00279654
Miat	0.00564358	0.000557471	0.00279654
Moxd1	0.00322311	0.000557471	0.00279654
Mpz	0.0366969	0.000557471	0.00279654
Myl1	0.0118497	0.000557471	0.00279654
Mylpf	0.00322311	0.000557471	0.00279654
Ntn4	0.0207794	0.000557471	0.0255991
Ntrk3	0.00322311	0.000557471	0.00483895
Papss2	0.00322311	0.000557471	0.00279654
Pi16	0.00322311	0.000557471	0.00279654
Pknox2	0.0482395	0.000557471	0.00279654
Pla2g7	0.00322311	0.000557471	0.00687234
Plppr4	0.00322311	0.000557471	0.00867114
Ppp2r2c	0.00322311	0.000557471	0.00279654
Prrx1	0.00322311	0.000557471	0.0320907
Ptpru	0.0078259	0.000557471	0.0197755
Ptprv	0.00322311	0.000557471	0.00279654

Sall1	0.00322311	0.000557471	0.0103526
Sbspon	0.00322311	0.000557471	0.0278322
Scin	0.00322311	0.00104026	0.0486371
Sfrp1	0.0174222	0.000557471	0.00483895
Slc16a3	0.0190842	0.000557471	0.00279654
Sost	0.0311323	0.000557471	0.00279654
Stc1	0.00322311	0.000557471	0.00279654
Steap1	0.00322311	0.000557471	0.0475736
Stk39	0.00322311	0.000557471	0.00483895
Stra6	0.00322311	0.000557471	0.00279654
Svep1	0.00322311	0.000557471	0.00279654
Tbx2	0.00564358	0.000557471	0.0103526
Tnn	0.00322311	0.000557471	0.00279654
Tnnc1	0.00564358	0.000557471	0.00279654
Tnnc2	0.00322311	0.000557471	0.00279654
Tnni1	0.0078259	0.000557471	0.00687234
Trabd2b	0.00322311	0.000557471	0.0475736
Ttc22	0.0207794	0.000557471	0.0278322
Tubb3	0.0222206	0.000557471	0.00279654
Vwf	0.00322311	0.000557471	0.0103526
Wipf3	0.00322311	0.000557471	0.04151
Wnt10a	0.00322311	0.00993085	0.0144358
Wnt16	0.00322311	0.000557471	0.0197755
Wnt5a	0.00322311	0.000557471	0.00483895
Xylt1	0.00564358	0.00962731	0.00279654
Zfp185	0.0416782	0.00189595	0.0364895

Table 3. Differentially expressed genes (q<0.05) and their corresponding q-values at ages P0 and P9, generated by DESeq

*denotes proximal > distal expression

Gene Name	*P0 q-value*	*P9 q-value*
Ano3	0.00654939886	0.0144428606
Apod*	0.00158825226	6.06E-10
Cacna2d2	7.01E-07	3.50E-05
Cbln2	0.00258213822	1.55E-20
Cdh10	0.0217872733	0.000435967632
Cdh18	8.16E-06	0.0102451015
Crabp1*	0.0164358384	0.000159870772
D030045P18Rik	0.00348699373	0.00588455423
Dpp6	0.00357832907	0.0278253141
Epha7	0.00142826128	0.0109620794
Eya1*	6.68E-14	0.00329849404
Galnt13	0.0389634776	0.00551707305
Gria4	4.22E-08	0.0122898617
Lhx9	3.21E-17	5.26E-10
Lmx1a	5.96E-07	0.0401636401
Lonrf2*	0.0117922378	0.000411140984
Magel2*	0.0267472585	0.000167049228
Mecom	0.0164358384	0.00405042489
Meis1	0.000162688158	0.0496802304
Ntrk3*	0.0142509219	0.0116498813
Pax9	7.75E-08	0.0140249058
Pi16*	0.000337077599	0.0355424143
Ppef1	0.000270473475	0.0159529844
Ppp2r2c*	0.000196621806	2.54E-09
Ptprv*	0.00798779048	0.0371636449
Sall1*	2.91E-35	1.55E-20

Sbspon*	9.68E-16	0.0496802304
Slc4a10	1.64E-05	0.00100835389
Slitrk5	0.000179553655	1.00E-04
Sorcs2	0.000481832645	0.0371882319
Stra6*	4.33E-12	1.55E-20
Syt9	0.0131171399	0.017259627
Tnn*	0.00187469108	2.22E-07
Wipf3*	0.00044603455	0.00101442022
Wnt10a*	0.0267472585	9.80E-09

Table 4. Differentially expressed genes (q<0.05), generated by both analysis pipelines, and their corresponding locations on the mm10 genome

Gene Name	*Location on mm10 genome*
Eya1	chr1:14168958-14310199
Sbspon	chr1:15853861-15892722
Lonrf2	chr1:38794508-38821215
Wnt10a	chr1:74792018-74804175
Ptprv	chr1:135108497-135132575
Tnn	chr1:160085031-160153575
Pppr2c2	chr5:36868569-36955078
Wipf3	chr6:54452883-54503768
Magel2	chr7:62376978-62381640
Ntrk3	chr7:78192113-78577838
Sall1	chr8:89027243-89044162
Crabp1	chr9:54764747-54773110
Stra6	chr9:58129349-58153997
Apod	chr16:31296191-31314808
Pi16	chr17:29318881-29328902

DISCUSSION

In the Methods chapter, I describe using a Galaxy pipeline to calculate q-values for the expression of each gene across three litters within each age group (P0, P4, and P9). Genes with significant differential expression were determined by a q-value range of $q < 0.05$. Tables 1 and 2 display the genes expressed at all three developmental ages. This is the working list of genes which show significant expression throughout the developmental time of metatarsal growth plate formation. In this chapter, I explore what we currently know about several of these genes and how their previously-studied functions may be related to a role in growth plate formation.

Sall1

Sall1 is a strong candidate for a signal of growth plate formation. At age P4, there is an extremely large difference in expression between locations, with higher expression observed on the proximal end. Its expression exhibits significance at all ages (P0, P4, and P9) with a q-value less than 0.05.

Kawakami, et al. (2009) have explored the relationship between Sall1 and Hox13 in limb morphogenesis. They describe an antagonistic relationship of "fine-tuning of local Hox activity that leads to proper morphogenesis of each cartilage element of the vertebrate autopod." While *Sall1* encodes a transcription factor, mutations to increase *Sall1* expression, did not alter Hox gene expression. They propose, rather than affecting Hox transcription, the Sall1 transcription factor competes with Hox proteins in binding to target sequences.

In a genome-wide analysis, Karantzali, et al. (2011) found 591 genes with binding loci for the Sall1 transcription factor. Many of these genes are related to cell differentiation and self-

renewal. Sall1 transcription factors regulate cell pluripotency in developing mouse embryos by targeting many of these genes to maintain pluripotency of particular cells (2011). The high expression difference seen in our data warrants further exploration into a possible role of Sall1 in preventing cell maturation and how this could be related to the differential expression observed in my analysis. As shown in Figure 4, *Sall1* expression was significantly greater on the proximal end of the metatarsal at both P0 and P9. The decreased *Sall1* expression on the distal end could be allowing for the chondrocyte maturation and formation of the secondary ossification center.

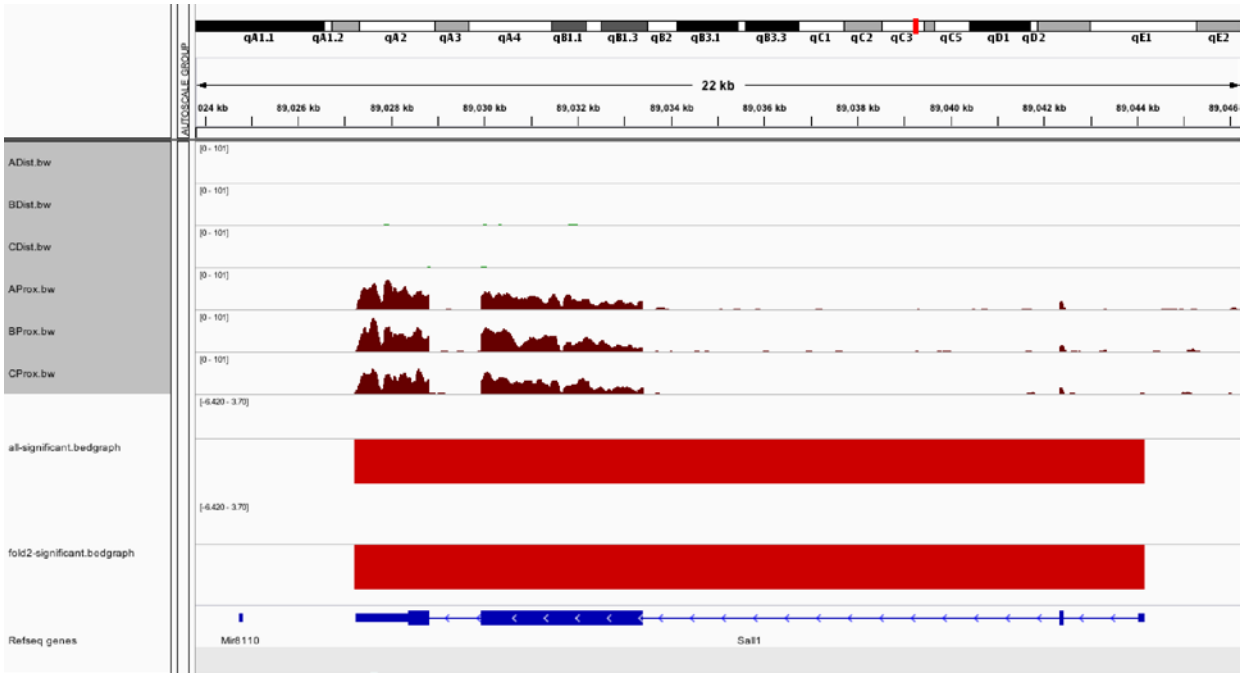

Figure 5. *Sall1* Expression at Age P4

Eya1

Eya1 expression patterns appear to be highly conserved across vertebrate species. Eya genes function as both transcription factors and phosphatases, allowing them control over many cellular processes. In vertebrates, Eya genes have been shown to play a role in mesenchyme differentiation. Eya1 and Six1 regulate peri-cloacal mesenchyme development and have an effect on *Fgf8* and *Bmp4* expression (Wang et al. 2011). Eya1 and Six1 also regulate neuron differentiation (Riddiford and Schlosser 2017), and Eya1 interacts with Notch signaling in craniofacial development (Zhang et al. 2017). Downregulation of *Eya1* is correlated with cell differentiation and decreases in plasticity.

Xu, et al. (1997) found evidence of Eya1 and Eya2 playing a role in limb connective tissue development. This study focused on expression in flexor vs. extensor tendon development and used subjects at ages prior to chondrocyte differentiation and ossification in the metatarsals. Most of the *Eya1* expression is seen in the mesenchyme surrounding the condensing cartilage and is concentrated on the ventral side. A study by Grifone et al. (2007) supports a role of Eya1 and Eya2 in myogenesis, while no effect on skeletal development is noted. However, a section at age E14.5 shows *Eya1* expression at two locations of joint formation appearing to correspond to the metacarpal-phalangeal joint (Xu et al. 1997). Further examination is needed to determine if the differential expression seen in my analysis is related solely to the surrounding connective tissue development or may be influencing the differential ossification of the metatarsal.

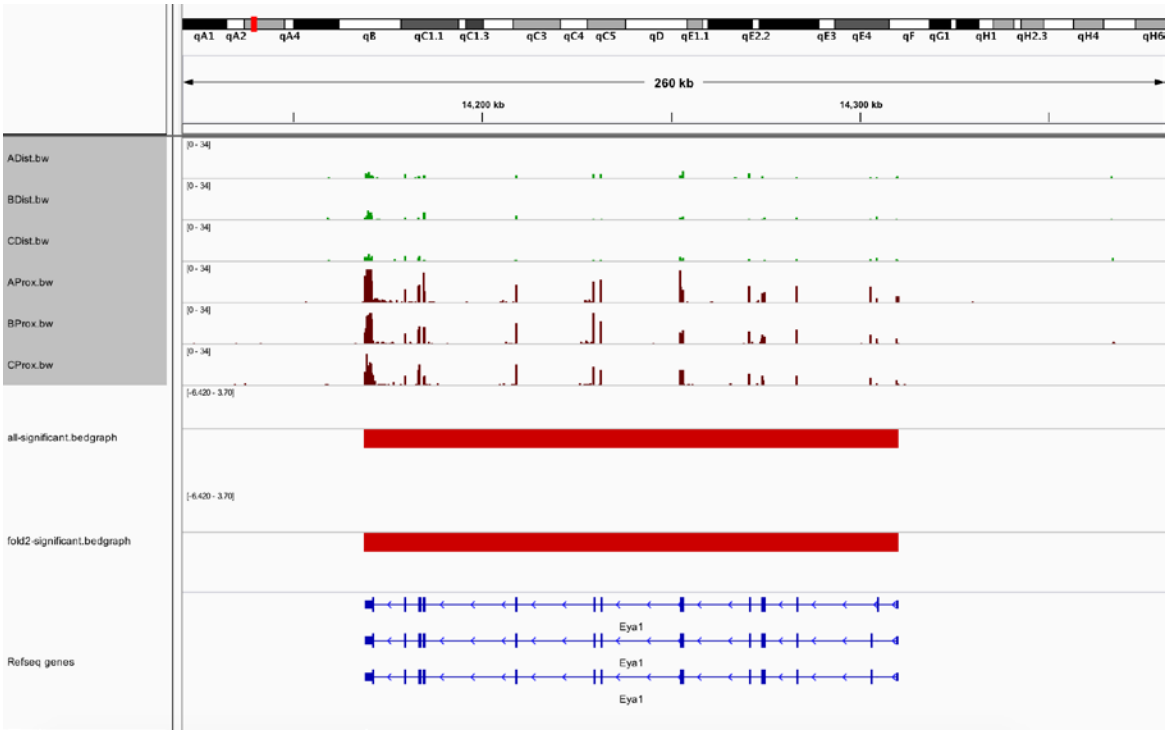

Figure 6. *Eya1* Expression at Age P4

Stra6

The *Stra6* gene codes for a cell surface receptor protein. This protein binds to a retinol-binding protein (Rbp4) to transport retinol into the cell (Blaner 2007). *Stra6* is expressed at blood-organ barriers and during the cell condensation of chondrogenesis (Bouillet et al. 1997). Retinoids, which are metabolized retinol, activate gene transcription and play a role in bone growth. Hatfield et al. (2012) used immunohistochemistry to observe *Rbp4* expression in the developing mouse hind limb. Rbp4 was found in hypertrophic chondrocytes just before formation of the secondary ossification center. They hypothesize Rbp4 stimulates the production of the vascular endothelial growth factor, which promotes cartilage remodelling and vascularization, and activates matrix-degrading enzymes (Hatfield, Anderson, and Powell 2012).

Chazaud et al. (1996) examined *Stra6* expression in the limb during prenatal development. *Stra6* expression shifted distally in early limb bud formation and became restricted to the perichondrium as the mesenchyme differentiated. Specifically, at embryonic age 16.5, *Stra6* was expressed in the perichondrium adjacent to the elongating cartilage of the femur, suggesting a role in cartilage differentiation into periosteum (Chazaud et al. 1996). Our analysis found *Stra6* differentially expressed in the distal, growth plate forming, end of the metatarsal. Immunohistochemistry of the postnatal metatarsal will show the pattern of *Stra6* expression later in development, around the time of secondary ossification center formation, and show the difference in expression between the two ends.

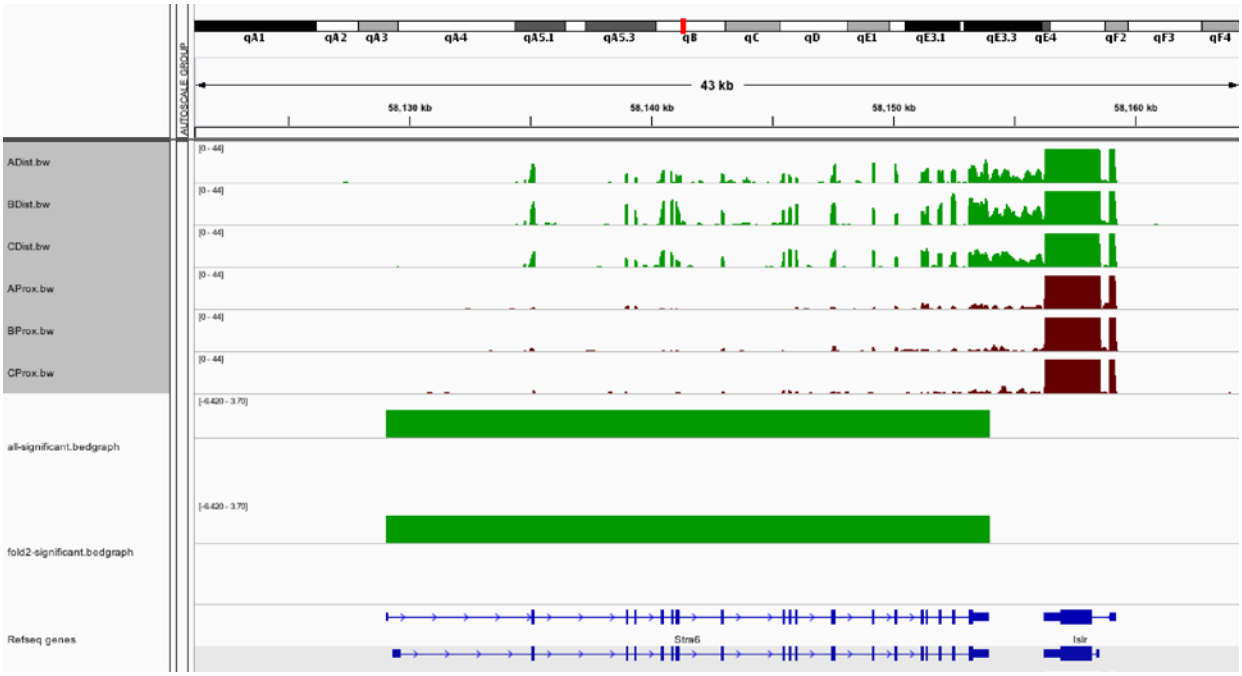

Figure 7. *Stra6* Expression at Age P4

Wnt

Wnt genes are known to interact with β-catenin to regulate developmental patterning. Between both statistical tests, *Wnt10a* was the only Wnt gene confirmed to be differentially expressed. The Galaxy test also detected differential *Wnt5a* and *Wnt16* expression across all ages. Cawthorn, et al. (2011) examined *Wnt6*, *Wnt10a*, and *Wnt10b* expression levels and patterning in differentiating mesenchyme. They concluded all three genes have an inhibiting effect on adipogenesis and stimulate mesenchyme differentiation into osteoblasts. A study by Andrade, et al. (2007) found evidence of elevated Wnt genes 2b, 4, 5a, 5b, 10b, and 11 in proximal tibial growth plates. Wnt10a was only detected in the growth plate in small amounts, which became negligible when broken down into particular tissues, so it was concluded that Wnt10a did not likely play a role in growth plate formation. Our data presented significantly higher expression in the non-growth plate forming end of the metatarsal. Further examination of Wnt10a patterning and function is needed to determine how this gene may play a role in the differentiation of ossification processes.

Most effects of Wnt10a are associated with ectodermal tissues, rather than mesoderm. During embryonic development, *Wnt10a* is expressed in the limb ectoderm, apical ectodermal ridge, and epidermal basal cell layer (Witte et al. 2009). Research suggests Wnt10a regulates odontoblast differentiation and dentinogenesis (Takashi et al. 2007), and mutations in Wnt10a cause a type of ectodermal dysplasia called odontoonychodermal dysplasia (Wang et al. 2014).

Missense mutations in Wnt5a are thought to cause Robinow syndrome, a form of dwarfism which causes shortened limbs, flattened facial formation, as well as other symptoms (Person et al. 2010). This supports a role of Wnt5a in skeletal development, especially longitudinal limb growth. During early foot joint formation (E11.5-E13.5), *Wnt16* is expressed in

the metatarsal-phalangeal joint in higher amounts than *Wnt4* and *Wnt14*. The latter two genes are expressed to a greater extent in the interphalangeal joints, while *Wnt16* is expressed in to a minor extent in these joints (Guo et al. 2004). A genome-wide association study of osteoporosis patients as well as a mouse gene deletion suggest *Wnt16* expression is directly correlated with cortical bone thickness and strength (Zheng et al. 2012). Dell'Accio et al. (2008) found upregulation of *Wnt16* after articular cartilage injury and in individuals with osteoarthritis, suggesting a regulatory role of Wnt16 in cartilage reconstruction. Wnt16 also may suppress osteoblast differentiation in intramembranous ossification (Zheng et al. 2013).

Lhx and Ihh

The Galaxy differential expression test detected a number of genes with previously known roles in limb development. A LIM homeobox domain (*Lhx9*) was more highly expressed in the distal region across all ages. During prenatal development, Lhx9, along with Lhx2 and Lhx1b, transcription factors are involved in anteroposterior and dorsoventral limb patterning. Early in development they are expressed throughout the limb bud, but become limited to distal regions by embryonic day 12. These factors may be activated by Wnt7a, and a knockout of both *Lhx2* and *Lhx9* in mouse embryos resulted in reduced *Ihh* expression in both the forelimb and hind limb, observed around embryonic days 10.5-11.5 (Tzchori et al. 2009). While Tzchori et al. (2009) focused on earlier stages of development, it is possible the LIM homeobox transcription factors have an effect on *Ihh* expression later in development. As described previously, Ihh plays a role in chondrocyte proliferation, organization, maturation, and differentiation into osteoblasts through the regulation of genes, such as *Bmp4*, *PTHrP*, and *RUNX2* (Long and Ornitz 2013). Ihh

also stimulates a sequence of expression events leading to the vascularization necessary for the formation of the secondary ossification center (Long and Ornitz 2013). Our findings of differential expression of both *Ihh* and *Lhx9* prompt further exploration into their interactions throughout limb development and potential roles in growth plate formation.

Gdf6

Growth and development factor-6 (Gdf6) is also termed bone morphogenic protein-13 (BMP-13) as well as cartilage-derived morphogenic protein-2 (CDMP-2). From the names alone, it is clear this protein plays a role in bone development and morphology. The differential expression of this gene was only determined to be significant by the Galaxy analysis, not by the DESeq test. Gdf6 protein coding region is just one gene in many BMP genes that play roles in skeletal development. While the others may be more commonly studied, Shen et al. (2009) propose a crucial role of Gdf-6 in controlling the differentiation of bone marrow multipotent mesenchymal stromal cells (BM MSCs). In their study, Shen et.al (2009) demonstrated this BMP's ability to prevent differentiation of BM MSCs into osteoblasts. In inhibiting osteoblast genesis, Gdf6 is regulating bone formation. Mutations in Gdf6 cause excessive bone growth, often leading to bone fusion in the wrist and ankle as well as in the vertebral column. Gdf6 also promotes genes responsible for BM MSCs development of a chondrogenic phenotype, as opposed to the osteogenic phenotype necessary for differentiating into an osteoblast.

CONCLUSION

Endochondral ossification is the process by which mesenchymal cells form a cartilage matrix as a precursor to bone formation. Some bones continue to maintain zones of replicating and maturing chondrocytes past embryonic development to allow for greater longitudinal growth throughout an individual's early life. This project revealed a plethora of candidate genes to be studied in terms of their functions and roles in endochondral ossification and growth plate formation. Use of in situ hybridization and immunohistochemical methods will reveal the expression patterns of these genes in the developing metatarsal. These are methods of probing for a specific mRNA transcript or translated protein and visualizing its locations on a tissue sample (Corthell 2014).

Developmental patterning relies on the timing and location of expressed genes. Changes to an organism's skeletal structure are the result of modifications to these patterns. Comparing patterns in the metatarsal to those in other bones, both growth plate-forming and non-growth plate-forming, will allow us to determine if these patterns are consistent across similar bone development morphologies. Additionally, it will be necessary to compare these patterns across vertebrate species. Studying homology in these genes and their expression between species may illuminate processes underlying evolutionary changes in bone morphology. Skeletons have evolved to provide structural support to vertebrates in different environments, protect variable internal organ systems, and allow for a variety of movement. From bipedal locomotion (Serrat et al. 2007) to precise grasping with our hands (Young 2003), humans have unique abilities, requiring morphological features which differ from our closest living relatives. By studying the molecular mechanisms underlying differential bone development, we hope to understand the processes by which new phenotypes arise in evolutionary history.

BIBLIOGRAPHY

Anders, Simon, and Wolfgang Huber

2010 Differential Expression Analysis for Sequence Count Data. Genome Biology 11(10): R106.

Andrade, Anenisia C, Ola Nilsson, Kevin M Barnes, and Jeffrey Baron

2018 Wnt Gene Expression in the Post-Natal Growth Plate: Regulation with Chondrocyte Differentiation. Bone 40(5). Elsevier: 1361–1369.

Blaner, William S.

2007 STRA6, a Cell-Surface Receptor for Retinol-Binding Protein: The Plot Thickens. Cell Metabolism 5(3). Cell Press: 164–166.

Bouillet, Philippe, Vincent Sapin, Claire Chazaud, et al.

1997 Developmental Expression Pattern of Stra6, a Retinoic Acid-Responsive Gene Encoding a New Type of Membrane Protein. Mechanisms of Development 63(2). Elsevier: 173–186.

Cawthorn, William P, Adam J Bree, Yao Yao, et al.

2012 Wnt6, Wnt10a and Wnt10b Inhibit Adipogenesis and Stimulate Osteoblastogenesis through a β-Catenin-Dependent Mechanism. Bone 50(2): 477–489.

Claire, Chazaud, Bouillet Philippe, Oulad-Abdelghani Mustapha, and Dollé Pascal

1998 Restricted Expression of a Novel Retinoic Acid Responsive Gene during Limb Bud Dorsoventral Patterning and Endochondral Ossification. Developmental Genetics 19(1). Wiley-Blackwell: 66–73.

Conesa, Ana, Pedro Madrigal, and Sonia Tarazona et al.

2016 A Survey Of Best Practices For RNA-Seq Data Analysis. Genome Biology 17(1). Springer Nature.

Corthell, John T.

2014 Basic Molecular Protocols in Neuroscience : Tips, Tricks, and Pitfalls. Elsevier Science.

Francesco, Dell'Accio, De Bari Cosimo, Eltawil Noha M, Vanhummelen Paul, and Pitzalis Costantino

2008 Identification of the Molecular Response of Articular Cartilage to Injury, by Microarray Screening: Wnt-16 Expression and Signaling after Injury and in Osteoarthritis. Arthritis & Rheumatism 58(5). Wiley-Blackwell: 1410–1421.

Gilbert, Scott F.

1991 Developmental Biology. New York: Plenum Press.

Grifone, Raphaelle, Josiane Demignon, Julien Giordani, et al.

2007 Eya1 and Eya2 Proteins Are Required for Hypaxial Somitic Myogenesis in the Mouse Embryo. Developmental Biology 302(2). Academic Press: 602–616.

Guo, Xizhi, Timothy F Day, Xueyuan Jiang, et al.

2004 Wnt/β-Catenin Signaling Is Sufficient and Necessary for Synovial Joint Formation. Genes & Development 18(19). Cold Spring Harbor Laboratory Press: 2404–2417.

Hatfield, Jodie T, Peter J Anderson, and Barry C Powell

2013 Retinol-Binding Protein 4 Is Expressed in Chondrocytes of Developing Mouse Long Bones: Implications for a Local Role in Formation of the Secondary Ossification Center. Histochemistry and Cell Biology 139(5): 727–734.

Karantzali, Efthimia, Vassilios Lekakis, Marilia Ioannou, et al.

2011 Sall1 Regulates Embryonic Stem Cell Differentiation in Association with Nanog. Journal of Biological Chemistry.

Kawakami, Yasuhiko

2009 Sall Genes Regulate Region-Specific Morphogenesis in the Mouse Limb by Modulating Hox Activities. Development 136: 585–594.

Kjosness, Kelsey M., Jasmine E. Hines, C. Owen Lovejoy, and Philip L. Reno

2014 The Pisiform Growth Plate Is Lost In Humans And Supports A Role For Hox in Growth Plate Formation. Journal Of Anatomy 225(5). Wiley-Blackwell: 527–538.

2017 The Pea-Shaped Human Pisiform Results From The Evolutionary Loss Of A Growth Plate. FASEB 27(1).

Long, Fanxin, and David M Ornitz

2013 Development of the Endochondral Skeleton. Cold Spring Harbor Perspectives in Biology 5(1). Cold Spring Harbor Laboratory Press: a008334.

Müller, Gerd B, and Stuart A Newman

2003 Origination Of Organismal Form. Cambridge, Mass.: MIT Press.

Person, Anthony D, Soraya Beiraghi, Christine M Sieben, et al.

2010 WNT5A Mutations in Patients with Autosomal Dominant Robinow Syndrome. Developmental Dynamics : An Official Publication of the American Association of Anatomists 239(1): 327–337.

Reno, Philip L., Denise L. Mcburney, C. Owen Lovejoy, and Walter E. Horton

2005 Ossification Of The Mouse Metatarsal: Differentiation And Proliferation In The Presence/Absence Of A Defined Growth Plate. The Anatomical Record Part A: Discoveries In Molecular, Cellular, And Evolutionary Biology 288A(1). Wiley-Blackwell: 104-118.

Reno, Philip L., Kelsey M. Kjosness, and Jasmine E. Hines

2016 The Role Of Hox In Pisiform And Calcaneus Growth Plate Formation And The Nature Of The Zeugopod/Autopod Boundary. Journal Of Experimental Zoology Part B: Molecular And Developmental Evolution 326(5). Wiley-Blackwell: 303-321.

Reno, Philip L., Walter E. Horton, Ruth M. Elsey, and C. Owen Lovejoy

2007 Growth Plate Formation And Development In Alligator And Mouse Metapodials: Evolutionary And Functional Implications. Journal Of Experimental Zoology Part B: Molecular And Developmental Evolution 308B(3). Wiley-Blackwell: 283-296.

Riddiford, Nick, and Gerhard Schlosser

2017 Six1 and Eya1 Both Promote and Arrest Neuronal Differentiation by Activating Multiple Notch Pathway Genes. Developmental Biology 431(2): 152–167.

Robinson, James T, Helga Thorvaldsdóttir, and Wendy Winckler et al.

2011 Integrative Genomics Viewer. Nature Biotechnology 29(1). Springer Nature: 24-26.

Roff, Derek A.

2006 Introduction To Computer-Intensive Methods Of Data Analysis In Biology. Cambridge: Cambridge University.

Serrat, Maria A, Philip L Reno, Melanie A McCollum, Richard S Meindl, and C. Owen Lovejoy

2007 Variation in Mammalian Proximal Femoral Development: Comparative Analysis of Two Distinct Ossification Patterns. Journal of Anatomy 210(3): 249–258.

Shen, Bojiang, Divya Bhargav, Aiqun Wei, et al.

2009 BMP-13 Emerges as a Potential Inhibitor of Bone Formation. International Journal of Biological Sciences 5(2): 192–200.

Soneson, Charlotte, and Mauro Delorenzi

2013 A Comparison of Methods for Differential Expression Analysis of RNA-Seq Data. BMC Bioinformatics 14(1): 91.

Takashi, Yamashiro, Zheng Li, Shitaku Yuko, et al.

2007 Wnt10a Regulates Dentin Sialophosphoprotein mRNA Expression and Possibly Links Odontoblast Differentiation and Tooth Morphogenesis. Differentiation 75(5). Wiley/Blackwell (10.1111): 452–462.

Trapnell, Cole, David G Hendrickson, and Martin Sauvageau et al.

2013 Differential Analysis Of Gene Regulation At Transcript Resolution With RNA-Seq. Nature Biotechnology 31(1). Springer Nature: 46-53.

Trapnell, Cole, Adam Roberts, and Loyal Goff et al.

2012 Differential Gene And Transcript Expression Analysis Of RNA-Seq Experiments With Tophat And Cufflinks. Nature Protocols 7(3). Springer Nature: 562-578.

Tzchori, Itai, Timothy F Day, Peter J Carolan, et al.

2009 LIM Homeobox Transcription Factors Integrate Signaling Events That Control Three-Dimensional Limb Patterning and Growth. Development (Cambridge, England) 136(8). Company of Biologists: 1375–1385.

Wang, Chen, Patricio Gargollo, Chaoshe Guo, et al.

2011 Six1 and Eya1 Are Critical Regulators of Peri-Cloacal Mesenchymal Progenitors during Genitourinary Tract Development. Developmental Biology 360(1). Academic Press: 186–194.

Wang, Yiping, Yi-Ping Li, Christie Paulson, et al.

2014 Wnt and the Wnt Signaling Pathway in Bone Development and Disease. Frontiers in Bioscience (Landmark Edition) 19: 379–407.

Wang, Zhe, Rebecca L Young, Huiling Xue, and Günter P Wagner

2011 Transcriptomic Analysis of Avian Digits Reveals Conserved and Derived Digit Identities in Birds. Nature 477. Nature Publishing Group, a division of Macmillan Publishers Limited. All Rights Reserved: 583.

Xu, Pin-Xian, Jane Cheng, Jonathan A Epstein, and Richard L Maas

1997 Mouse Eya Genes Are Expressed during Limb Tendon Development and Encode a Transcriptional Activation Function. Proceedings of the National Academy of Sciences 94(22): 11974.

Young, Richard W.

2003 Evolution of the Human Hand: The Role of Throwing and Clubbing. Journal of Anatomy 202(1). Wiley/Blackwell (10.1111): 165–174.

Zhang, Haoran, Li Wang, Elaine Yee Man Wong, et al.

2017 An Eya1-Notch Axis Specifies Bipotential Epibranchial Differentiation in Mammalian Craniofacial Morphogenesis. Marianne Bronner, ed. eLife 6. eLife Sciences Publications, Ltd: e30126.

Zhang, Zong Hong, Dhanisha J Jhaveri, Vikki M Marshall, et al.

2014 A Comparative Study of Techniques for Differential Expression Analysis on RNA-Seq Data. PLOS ONE 9(8). Public Library of Science: e103207-.

Zheng, Hou-Feng, Jon H. Tobias, Emma Duncan, et al.

2012 WNT16 Influences Bone Mineral Density, Cortical Bone Thickness, Bone Strength, and Osteoporotic Fracture Risk. Greg Gibson, ed. PLoS Genetics 8(7). Public Library of Science: e1002745.

Zheng, Jiang, Von den Hoff Johannes W, Torensma Ruurd, Meng Liuyan, and Bian Zhuan

2013 Wnt16 Is Involved in Intramembranous Ossification and Suppresses Osteoblast Differentiation Through the Wnt/β-Catenin Pathway. Journal of Cellular Physiology 229(3). Wiley-Blackwell: 384–392.

Zheng, Zhengui, and Martin J Cohn

2011 Developmental Basis of Sexually Dimorphic Digit Ratios. Proceedings of the National Academy of Sciences of the United States of America 108(39). National Academy of Sciences: 16289–94.